4108–4119 *Nucleic Acids Research, 2010, Vol. 38, No. 12* *Published online 9 March 2010*
doi:10.1093/nar/gkq151

Cleavage of the sarcin–ricin loop of 23S rRNA differentially affects EF-G and EF-Tu binding

Lucía García-Ortega[1,2], Elisa Álvarez-García[1,2], José G. Gavilanes[2], Álvaro Martínez-del-Pozo[2] and Simpson Joseph[1,*]

[1]Department of Chemistry and Biochemistry, University of California at San Diego, La Jolla, CA 92093, USA and [2]Departamento de Bioquímica y Biología Molecular I, Universidad Complutense, 28040 Madrid, Spain

Received November 24, 2009; Revised February 18, 2010; Accepted February 19, 2010

ABSTRACT

Ribotoxins are potent inhibitors of protein biosynthesis and inactivate ribosomes from a variety of organisms. The ribotoxin α-sarcin cleaves the large 23S ribosomal RNA (rRNA) at the universally conserved sarcin–ricin loop (SRL) leading to complete inactivation of the ribosome and cellular death. The SRL interacts with translation factors that hydrolyze GTP, and it is important for their binding to the ribosome, but its precise role is not yet understood. We studied the effect of α-sarcin on defined steps of translation by the bacterial ribosome. α-Sarcin-treated ribosomes showed no defects in mRNA and tRNA binding, peptide-bond formation and sparsomycin-dependent translocation. Cleavage of SRL slightly affected binding of elongation factor Tu ternary complex (EF-Tu•GTP•tRNA) to the ribosome. In contrast, the activity of elongation factor G (EF-G) was strongly impaired in α-sarcin-treated ribosomes. Importantly, cleavage of SRL inhibited EF-G binding, and consequently GTP hydrolysis and mRNA–tRNA translocation. These results suggest that the SRL is more critical in EF-G than ternary complex binding to the ribosome implicating different requirements in this region of the ribosome during protein elongation.

INTRODUCTION

Ribotoxins are a family of toxic extracellular fungal ribonucleases (RNases) that exert an exquisite ribonucleolytic activity on the larger rRNA, leading to protein synthesis inhibition and cell death by apoptosis (1). α-Sarcin, a well-studied ribotoxin, cleaves the phosphodiester bond between G2661–A2662 located in helix 95 of 23S rRNA (1–4) (Figure 1A and B). Helix 95 is also targeted by ricin, a *N*-glycosidase that inactivates the ribosome by depurinating A2660 (5). Hence helix 95 of 23S rRNA is known as the sarcin–ricin loop (SRL). The SRL comprises one of the longest stretches of universally conserved rRNA sequence indicating a crucial role in protein synthesis (2654–2665 in *Escherichia coli* 23S rRNA). Consistent with an important functional role, mutations or deletions in the SRL sequence are lethal (6–8).

The SRL together with the GTPase-associated center (GAC, helices 43 and 44 of 23S rRNA) form the main interaction site for EF-G and EF-Tu with the rRNA in the large ribosomal subunit (9,10). More recently, studies have shown that *E. coli* initiation factor 2 (IF2) and release factor 3 (RF3) interact with the same region of the ribosome (10). In general, all these proteins are GTPases that bind to the ribosome, hydrolyze GTP and undergo conformational changes before dissociating from the ribosome. A challenging problem is to understand how the ribosome regulates the association of specific factors during defined steps of protein biosynthesis.

Three major steps occur during protein elongation (11). First, a ternary complex formed by EF-Tu, GTP and the cognate aminoacyl-tRNA binds to the A site of the ribosome carrying either an initiator fMet-tRNA^{fMet} or peptidyl-tRNA in the P site. EF-Tu•GDP dissociates from the ribosome and the aminoacyl-tRNA is accommodated into the A site. In the second step, the ribosome catalyzes the peptidyl transferase reaction, resulting in a deacylated tRNA at the P site and a peptidyl-tRNA at the A site. The cycle is completed by the translocation of the tRNAs catalyzed by EF-G. After translocation and release of EF-G, the ribosome repeats the elongation cycle until a stop codon is encountered. The entry of a stop codon into the A site signals the termination of protein synthesis.

Biochemical studies as well as structural data have helped to elucidate the role of GTP hydrolysis by EF-Tu and EF-G. During tRNA selection by the ribosome,

*To whom correspondence should be addressed. Tel: +1 858 822 2957; Fax: +1 858 534 7042; Email: sjoseph@ucsd.edu

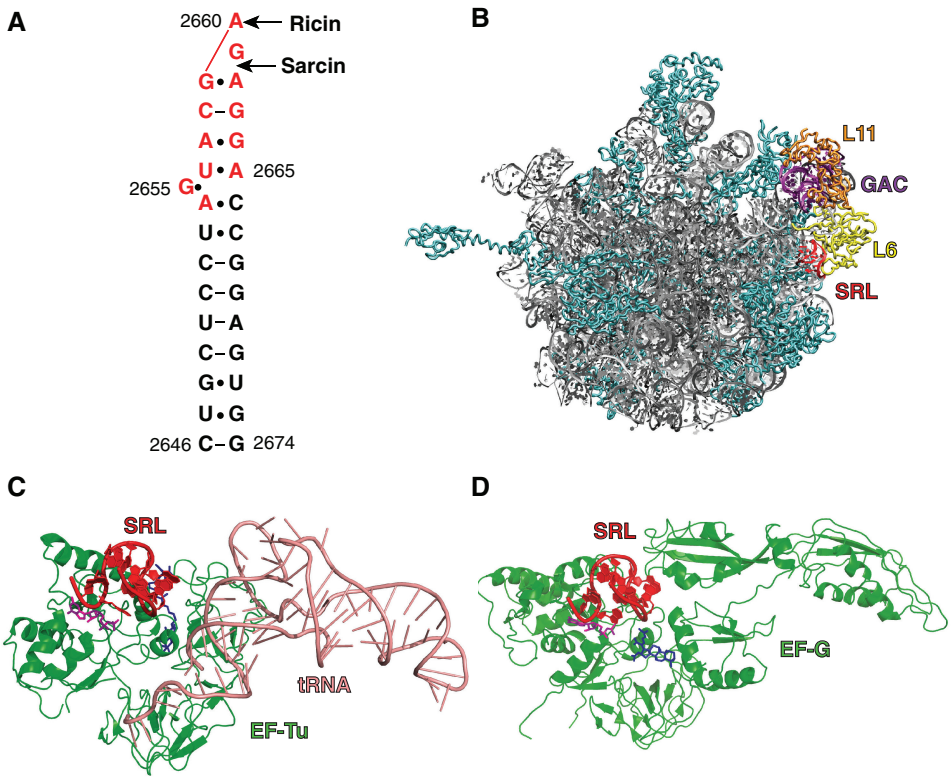

Figure 1. Interaction of EF-Tu ternary complex and EF-G with the SRL. (**A**) Secondary structure of the SRL. The universally conserved bases in the SRL are shown in red. The sites of cleavage by α-sarcin and modification by ricin are indicated by the arrows. (**B**) The X-ray crystal structure of the *E. coli* 50S ribosomal subunit (PDB accession code 2aw4). The rRNAs are represented by the grey ribbons and the ribosomal proteins by cyan tubes. Indicated are the SRL (red), GAC (purple), ribosomal proteins L6 (yellow) and L11 (orange). (**C**) The interaction of EF-Tu ternary complex with the SRL (PDB accession codes 2wrn and 2wro). Shown are the SRL (red), EF-Tu (green), GDP (magenta), kirromycin (blue) and tRNA (salmon). (**D**) The interaction of EF-G•GDP with the SRL (PDB accession codes 2wri and 2wrj). Shown are the SRL (red), EF-G (green), GDP (magenta), and fusidic acid (blue).

codon recognition triggers GTP hydrolysis by EF-Tu that catalyzes the accommodation of the tRNA into the A site (12). In the case of EF-G, GTP hydrolysis induces conformational changes in the ribosome, that allow the disruption of the interactions between the A site tRNA and the small subunit decoding center promoting a rapid translocation of the mRNA–tRNA complex (13–16). It has been suggested that GTP hydrolysis by EF-Tu and EF-G is triggered by ribosomes in two different conformational states corresponding to the different steps in the elongation cycle (17,18). How binding of EF-G and EF-Tu to the ribosome triggers GTP hydrolysis is still not clear. Cryo-EM data showed that the SRL interacts intimately with the GTPase domain of EF-Tu (19,20) and EF-G (16,21) implying that the SRL plays an important role during GTP hydrolysis. Consistent with the cryo-EM data, recent X-ray crystal structures of EF-Tu ternary complex (22) and EF-G (23) bound to the ribosome showed that the SRL is indeed positioned close to GTPase domain in both structures (Figure 1C and D). The SRL appears to interact with EF-Tu and EF-G without undergoing any significant change in its conformation. Since the EF-G bound complex represents the post-translocation state, it is not clear from the X-ray crystal structures how the SRL may regulate the binding of these factors during the elongation cycle.

Interestingly, Nierhaus and co-workers showed that cleavage of the SRL by α-sarcin modestly affected the binding of EF-Tu ternary complex, while the binding of EF-G and translocation were strongly inhibited (4). However, recent studies suggest that the SRL may play a more specific role in EF-G and EF-Tu function. For example, G2655C mutation in the SRL, which was lethal and strongly inhibited translocation, only moderately affected binding of EF-G and GTPase activity (24). Additionally, a single-molecule study showed that ribosomes treated with the α-sarcin homolog, restrictocin, were able to bind ternary complex and progress up to the GTPase-activated state (25). Thus, in some instances, EF-G and EF-Tu can bind to the ribosome with an inactive SRL.

In order to further explore the importance of the SRL for the elongation step of protein synthesis, we cleaved the SRL with α-sarcin. Conditions were optimized to get a more uniform extent of cleavage by α-sarcin and the level of cleavage was quantitated precisely by primer extension analysis. Consistent with the earlier study (4), our results show that cleavage of the SRL has modest effects on ternary complex binding, while more significantly affecting EF-G binding, GTP hydrolysis and translocation. These results confirm that, unlike EF-Tu ternary complex, EF-G requires an intact SRL for stably binding to the

ribosome. Interestingly, EF-G-independent translocation, induced by sparsomycin, is not affected indicating that the SRL is not required for the movement of the mRNA–tRNA complex in the ribosome.

MATERIALS AND METHODS

Preparation of ribosomes, mRNAs, tRNAs, elongation factors and α-sarcin

Tightly coupled 70S ribosomes were isolated from *E. coli* MRE 600 cells in mid-log phase and purified by sucrose density gradient (26). Phage T4 gene 32 mRNA was transcribed by T7 RNA polymerase from a linearized plasmid containing the appropriate insert. mRNA + 9 was purchased from Dharmacon and labelled at the 3′-end with pyrene succinimide as described (27). EF-Tu, EF-Tu H84A and EF-G were overexpressed and purified as native forms using the IMPACT system (New England Biolabs) (28). *E. coli* PheRS, MetRS and Methionyl-$tRNA^{fMet}$ formyltransferase were produced as recombinant proteins with His-tag to facilitate their purification. Native *E. coli* $tRNA^{fMet}$ and $tRNA^{Phe}$ were purchased from Sigma and aminoacylated and purified as described before (29). *Aspergillus giganteus* natural α-sarcin was produced, isolated to homogeneity and characterized as described previously (30).

Treatment with α-sarcin

Cleavage of 70S ribosomes by α-sarcin was assayed in four different buffers. Buffer A: 20 mM Hepes–KOH (pH 7.6), 8 mM $MgCl_2$, 150 mM NH_4Cl, 4 mM 2-mercaptoethanol, 0.05 mM spermine and 2 mM spermidine (31). Buffer B (A without polyamines): 20 mM Hepes–KOH (pH 7.6), 8 mM $MgCl_2$, 150 mM NH_4Cl, and 4 mM 2-mercaptoethanol. Buffer C (B with 6 mM EDTA): 20 mM Hepes–KOH (pH 7.6), 8 mM $MgCl_2$, 150 mM NH_4Cl, 4 mM 2-mercaptoethanol, and 6 mM EDTA. Buffer D (B with 8 mM EDTA): 20 mM Hepes–KOH (pH 7.6), 8 mM $MgCl_2$, 150 mM NH_4Cl, 4 mM 2-mercaptoethanol, and 8 mM EDTA. Different toxin concentrations and time of incubation were also tried. The highest efficiency of specific cleavage without non-specific degradation was obtained when 0.6 μM isolated 70S ribosomes were incubated with 0.3 μM α-sarcin during 30 min at 37°C in buffer C. These conditions were used for cleaving the SRL in all subsequent experiments (α-sarcin-treated ribosomes). Intact ribosomes were also incubated without α-sarcin. A small increase in EDTA concentration from 6 mM (buffer C in Figure 1D) to 8 mM (buffer D in Figure 1D) made the ribosomes more susceptible to non-specific cleavage.

Most translation experiments involving prokaryotic ribosomes were usually performed in the polyamine buffer (buffer A). When the functionality of cleaved ribosomes was studied, standard buffer conditions were restored and activation of ribosomes was performed (incubation at 42°C for 10 min and slow cool down to 37°C followed by an additional incubation for another 10 min at 37°C).

The integrity of α-sarcin cleaved ribosomes, before and after the functional assays was assessed by estimating their protein and rRNA content. The rRNA was phenol extracted and separated on a 2% agarose gel. The result was visualized by ethidium bromide staining. For protein content, ribosomes were separated from unbound proteins by filtration in 100 KDa MWCO Microcon spin filters (Amicon). Bound and unbound fractions were analyzed by 17% SDS–PAGE and coomassie blue staining.

Primer extension analysis

The extent and site of α-sarcin cleavage was determined by primer extension. Reverse transcription using the primer 5′-ACCAGTGATGCGTCCACTCCG-3′, complementary to the sequence 2634–2665 of *E. coli* 23S RNA (Figure 1B), and a mixture of dNTPs (−dATP) + ddATP, gave different products for an intact and a cleaved template. The uncleaved rRNA was transcribed up to the first uridine in the sequence due to the ddATP in the extension mixture (U2656). The extension with the α-sarcin cleaved template stopped at the cleavage site. The products of reverse transcription were separated in a 15% denaturing polyacrylamide gel and quantitated with a PhosphorImager (Molecular Dynamics).

In vitro translation assay

The overall activity of cleaved ribosomes was determined by an *in vitro* translation assay. Plasmid pRL-null (Promega) was modified by inserting a Shine–Dalgarno sequence (5′-**AAGGAGA**TATACAT**ATG**-3′) upstream of the start codon of the *Renilla* luciferase gene. The plasmid was linearized with Bam HI and used as the template for coupled transcription and translation of the luciferase gene *in vitro*. The linearized plasmid (1μg) was mixed with 8 μl of synthesis mix (200 mM Hepes-KOH, pH 8.2, 7 mM DTT, 4 mM ATP, 3.3 mM of CTP, GTP and UTP, 0.1 M phosphoenolpyruvate, 7.5% PEG-6000, 0.13 mg/ml folinic acid, 240 U/ml pyruvate kinase, 0.14 M NH_4Ac, 0.28 M KAc), 4 μL of 100 mM $MgCl_2$, 4 μl of *E. coli* S100 extract and T7 RNA polymerase. This mix was incubated for 45 min at 37°C to produce excess of mRNA for the assay. Then, 2 μl of 55 mM methionine, 6 μg of total tRNA from *E. coli* and 4 μl of 50 μM coelenterazine were added. The final volume of the reaction mixture was 55 μl. Activated ribosomes were prepared separately in standard buffer (6 pmol in 20 μl) and then combined with the reaction mixture and transferred to a 96-well plate. α-Sarcin treatment was performed either before the activation of the ribosomes or simultaneously with the translation reaction. The plate was incubated at 37°C in a plate reader (Genios, Tecan) and the synthesis of luciferase enzyme was monitored in real-time by measuring the luminescence every 90 s.

Peptidyl-transferase assay

The assay was performed essentially as described (32). f[^{35}S]Met-$tRNA^{fMet}$ was obtained by aminoacylation and formylation of $tRNA^{fMet}$ in the presence of [^{35}S]Met. Initiation complexes (ribosomes with mRNA and initiator tRNA in P site) were formed by incubating

activated 70S ribosomes (0.15 μM final concentration) with a 142 nucleotide fragment of gene 32 mRNA (0.3 μM final concentration) for 15 min at 37°C followed by the addition of f[^{35}S]Met-tRNA^{fMet} (0.25 μM final concentration) and further incubation for another 20 min. A-site was filled with Phe-tRNA^{Phe} or ternary complex (0.4 μM final concentrations) for different times at room temperature. Ternary complex binding should be completed in a second time scale, whereas factor-independent binding is a very slow process (in minutes). EF-Tu ternary complex was formed by incubating 9 μM EF-Tu with 1 mM GTP, 1 μl pyruvate kinase (10 mg/ml) and 3 mM phosphoenolpyruvate for 30 min at 37°C, then adding 3 μM Phe-tRNA^{Phe} and incubating again for 15 min at 37°C. The excess of EF-Tu present in the reaction ensures that all the Phe-tRNA^{Phe} is bound as EF-Tu ternary complex. Formation of fMet-Phe dipeptide was initiated by the addition of Phe-tRNA^{Phe} or ternary complex and stopped at different times with 1/5 volumes of 1 M KOH and placed on ice. The pH of the reaction mixture was neutralized and 1.5 μl aliquots were analyzed by electrophoretic TLC as described before (32). The amount of f[^{35}S]Met-Phe and f[^{35}S]Met were quantitated using a PhosphorImager (Molecular Dynamics). The dipeptide formed was about 30% of the total f[^{35}S]Met-tRNA^{fMet} added, so about 50% of the ribosomes were active for this assay. The fraction of dipeptide calculated per sample was normalized to the maximum formed with intact ribosomes in each experiment.

Translocation assays

Standard toeprinting assays for translocation were performed in standard polyamine buffer A as described before (33). Final concentrations were 0.15 μM ribosomes, 0.3 μM gene 32 mRNA fragment hybridized with 5′-[^{32}P]-AL2 primer, 0.35 μM tRNA^{fMet} or fMet-tRNA^{fMet} for the P site and 0.5 μM of tRNA^{Phe} or Phe-tRNA^{Phe} for the A site. After the addition of EF-G•GTP (1.2 μM EF-G and 1 mM GTP final concentrations) aliquots were stopped after 10 min at room temperature by placing them on ice. The sparsomycin-induced translocation was performed according to Fredrick and Noller (34). Ribosomes programmed with mRNA301 contained tRNA$_2^{Tyr}$ in the P site *N*-acetyl-Phe-tRNA^{Phe} in the A site. Translocation was induced by adding 0.5 mM sparsomycin (final concentration). For the time course analyses, aliquots were withdrawn at the various time points and mixed with viomycin (1 mM final concentration) to stop the reaction. Reverse transcription and gel analysis followed standard procedures (33). The gels were quantitated using a PhosphorImager (Molecular Dynamics).

Steady-state fluorescence measurements were also used to analyze translocation (27). Activated ribosomes (0.25 μM) were incubated with a 21 nucleotide pyrene-modified mRNA + 9 (0.5 μM) for 10 min at 37°C. Pre-translocation complexes were formed by adding fMet-tRNA^{fMet} (0.5 μM) and incubated for 20 min at 37°C followed by Phe-tRNA^{Phe} (0.6 μM) for another 20 min. Post-translocation complexes were obtained by adding 10 μl of EF-G•GTP mix (0.8 μM and 1 mM, respectively, final concentrations) to the pre-translocation complexes and incubating at 25°C for 15 min. Samples were excited at 343 nm and the emission spectrum of pyrene from 360 to 420 nm was recorded at 25°C with a photon-counting fluorometer (Fluoromax-P, JY Horiba). Translocation was followed by the decrease in fluorescence emission intensity at 376 nm (27).

EF-G-dependent GTP hydrolysis

Activated ribosomes (0.2 μM final concentration) were mixed with EF-G (from 1 to 9 μM final concentration) and GTP (1 mM final concentration with traces of [γ-^{32}P]-GTP, specific activity 25 Ci/mmol) at room temperature. Aliquots at different times were quenched with 5% SDS (1.25% final concentration). One microliter samples were spotted on PEI cellulose TLC plates and developed in 0.5 M KH_2PO_4 (pH 3.5). The amount of $^{32}P_i$ formed was quantitated using a PhosphorImager (Molecular Dynamics). The initial velocities (as GTP hydrolyzed per ribosome per second) were plotted versus each EF-G concentration and fitted to a Michaelis–Menten equation. The analysis of the data gave k_{cat}, K_M and k_{cat}/K_M kinetic constants of intact and 75% α-sarcin-cleaved ribosomes. The parameters for a population containing only α-sarcin-cleaved ribosomes were obtained according to Saarma *et al.* (35), using the equations:

$$\frac{k_{catsar}}{K_{Msar}} = \frac{[(k_{catmix}/K_{Mmix}) - (1-0.75)(k_{catWT}/K_{MWT})]}{0.75}$$

$$K_{Msar} = \frac{0.75}{[(1/K_{Mmix}) - (1-0.75)/K_{MWT}]}$$

Where sar, mix and WT stand for pure cleaved ribosome population, cleaved ribosomes contaminated with 25% of intact ribosomes, and intact ribosomes, respectively.

EF-G and EF-Tu-ternary complex binding to ribosomes

Binding of EF-G and EF-Tu ternary complex to the ribosome was analyzed by filtration (36). For EF-G binding, activated ribosomes (0.2 μM final concentration) were formed in standard polyamine buffer in 60 μl volume. Then, 20 μl of EF-G solution (minimum of 0.4 μM final concentration) with GTP or GDPNP (1 mM final concentration) were added to the reaction and incubated for 5 min at room temperature before filtering. For ternary complex binding, initiation complexes were formed in 60 μl final volume (0.2 μM ribosomes, 0.4 μM gene 32mRNA fragment and 0.4 μM fMet-tRNA^{fMet,} final concentrations). EF-Tu (or EF-Tu H84A) ternary complex was formed by incubating 1.6 μM of elongation factor with 4 mM GTP (or GDPNP) for 45 min at 37°C, then adding 2 μM Phe-tRNA^{Phe} and incubating again for 15 min at 37°C. Twenty microliters of ternary complex (0.4 μM final concentration) in the presence or absence of the antibiotic kirromycin (25 μM final concentration) were added and incubated for 5 min at room temperature. Unbound EF-G or ternary complex was removed using

100 000 MWCO Microcon spin filters (Amicon) and washing the samples twice with 300 µl of buffer containing the corresponding nucleotide and antibiotic. The washed samples were concentrated to 10 µl and analyzed by SDS–PAGE. The gels were scanned and the amount of factor bound to the ribosome was determined relative to the ribosomal protein S1 using ImageQuant (Molecular Dynamics).

RESULTS

Inactivation of *E. coli* ribosomes by α-sarcin

It is assumed that *E. coli* ribosomes are less susceptible to α-sarcin cleavage than their eukaryotic counterparts, although it is worth saying that comparison in exact same conditions has not yet been performed (2,3). Previous studies have reported inactivation of *E. coli* ribosome preparations ranging from 10 to 50% (4). Thus, our first goal was to optimize the inactivation procedure and minimize the contamination with intact ribosomes. Consequently, different buffers, concentration of reagents and time courses for the cleavage reaction were assayed. Primer extension was used to quantify the extent of cleavage and agarose gel electrophoresis was used to analyze the specificity of the cleavage and the integrity of the rRNA after treatment with the toxin (Figure 2A and B). The buffers tested were variations of the polyamine buffer (buffer A in Figure 2A) since this would be the one employed in subsequent functional assays (31). Previous reports indicated that the presence of millimolar concentrations of mono or divalent cations inhibited the ribonucleolytic activity of α-sarcin (37,38). Therefore, we tested variations of the buffer containing different concentrations of magnesium and polyamines. We tested buffer A without polyamines (buffer B), and decreased the magnesium concentration to 2 mM (buffer C) or to 0 mM (buffer D) by adding EDTA (see the 'Materials and Methods' section). We obtained 75% specifically cleaved ribosomes in buffer C, which contained 2 mM magnesium, no polyamines and 0.3 µM α-sarcin. Increasing the α-sarcin concentration or completely eliminating magnesium (buffer D) in the reaction resulted in additional cleavages other than that producing the specific α-fragment (Figure 2B). Thus, in our hands the best conditions gave 75% of specifically cleaved ribosomes and these were used for future experiments (Figure 2A). Ribosome requires a minimum concentration of magnesium and/or polyamines, so these were restored after α-sarcin treatment for functional assays (31).

Interestingly, the most efficient conditions gave a slightly different specificity with respect to the position of cleavage in the 23S rRNA. The expected cleavage is at the 3′ side of G2661 resulting in the primer extension stop at position A2662 (Figure 2A). However, an additional band appeared at position G2661 due to cleavage at the 3′ side of A2660. Close inspection of previous published results revealed a similar heterogeneity in the cleavage of *E. coli* ribosomes (6,39). Most probably this second cleavage site corresponded to a less specific action of the toxin since the conditions employed were drastic, which might have affected the conformation of the SRL.

In *vitro* translation is inhibited by cleaving the SRL

Protein composition of the α-sarcin-treated ribosomes was analyzed to determine whether cleavage of the SRL caused loss of ribosomal proteins. This was accomplished by filtering α-sarcin-treated ribosomes to separate possible unbound ribosomal proteins. The filtered fractions were then analyzed by SDS–PAGE (Figure 2C). Both untreated control ribosomes and α-sarcin-treated ribosomes showed similar levels of ribosomal proteins indicating no significant loss of proteins due to cleavage of the SRL. Although this electrophoresis cannot resolve all the ribosomal proteins, proteins L6, L11 and L14 that bind close to the SRL and are more likely to be affected by the action of α-sarcin, have molecular weights within the resolution range of the gel. These proteins were present at similar levels in the α-sarcin-treated ribosomes. Supporting this conclusion, no proteins were found in the filtrate besides α-sarcin.

Next, the ability of α-sarcin-treated ribosomes to bind aminoacylated tRNAs to the A site without the help of EF-Tu was determined. Ribosomes programmed with a defined mRNA and f-[^{35}S]Met-tRNA^{fMet} in the P site were incubated with Phe-tRNA^{Phe}. The amount of f-[^{35}S]Met-Phe dipeptide formed corresponds to the amount of Phe-tRNA^{Phe} bound to the A site. Dipeptides formed by the ribosome were separated by electrophoretic TLC (eTLC) and quantitated (Figure 2D). The extent of dipeptide formed was similar with untreated control ribosomes and α-sarcin-treated ribosomes. Thus, the intrinsic ability of the ribosomes to bind mRNA and tRNAs, and catalyze peptide bond formation in a factor-independent manner, was not impaired by cleaving the SRL.

The activity of α-sarcin-treated ribosomes was further studied using an *in vitro* translation assay, which monitors the synthesis of the reporter protein *Renilla* luciferase in a cell-free system (Figure 2E). When ribosomes were treated with α-sarcin before being added to the translation mixture, 75% inhibition of luciferase biosynthesis was observed in agreement with the efficiency of cleavage by α-sarcin. The addition of α-sarcin to the translation mixture without previous inactivation of the ribosomes did not affect the reaction indicating that at its final concentration α-sarcin did not show any degradation of rRNAs, mRNAs and tRNAs.

EF-Tu binding is not completely inhibited by cleaving the SRL

A previous study showed that cleaving the SRL did not affect the initial binding of the ternary complex to the ribosome but stalled the accommodation of the tRNA into the A site (25). We tested binding of the ternary complex to the ribosome using the dipeptide assay described above (Figure 3A). In order to ensure EF-Tu-dependent tRNA binding, a 3-fold molar excess

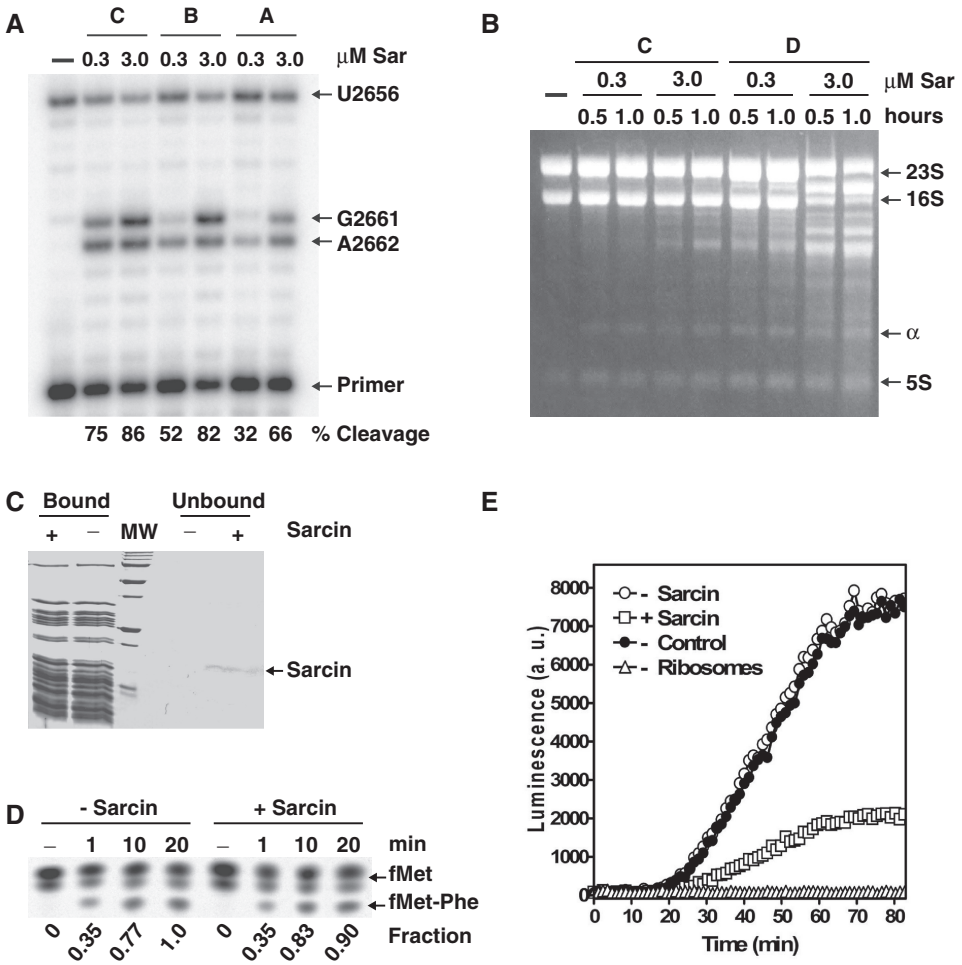

Figure 2. Effect of α-sarcin cleavage on ribosome structure and activity. (**A**) Primer extension analysis of 23S rRNA after cleavage by α-sarcin. Cleavage of *E. coli* ribosomes in buffers A, B (A minus polyamines) and C (B + 6mM EDTA) for 30 min with 0.3 or 3 μM α-sarcin. Control reaction without α-sarcin is indicated by (–). The arrows indicate the position in the 23S rRNA where the reverse transcription stops. The cleavage efficiency is indicated below the lanes. (**B**) Agarose gel electrophoresis of rRNAs extracted from α-sarcin-treated ribosomes. The cleavage reaction was performed in buffers C and D (B + 8 mM EDTA) with 0.3 or 3 μM α-sarcin and the reaction was incubated for 0.5 or 1 h as indicated above the lanes. Control reaction without α-sarcin is indicated by (–). 23S, 16S, 5S rRNA molecules and α-fragment are indicated by the arrows. (**C**) Protein profile of untreated control (–) and α-sarcin-treated (+) ribosomes. Proteins bound to the ribosome (bound) and free in solution (unbound) were separated by filtration and analyzed by SDS–PAGE. Position of α-sarcin (17 000 Da) is indicated by the arrow. MW represents protein standards from 250 to 10 KDa. (**D**) Non-enzymatic binding of tRNA and peptidyl transferase reaction. Time course of dipeptide formation with untreated (−Sarcin) and α-sarcin-treated ribosomes (+Sarcin). The products were separated by electrophoretic TLC and the dipeptide formed (fMet-Phe) is indicated by the arrow. The amount of dipeptide formed was normalized with respect to the amount formed by intact ribosomes after 20 min. Normalized fraction of dipeptide obtained is indicated below the lanes. (**E**) *In vitro* translation. Synthesis of luciferase reporter enzyme by untreated ribosomes (open circles) and ribosomes cleaved with α-sarcin (open squares). A control reaction with α-sarcin added to the translation mixture was performed for any non-specific activity (filled circles). In addition, a reaction without ribosomes was used as a negative control (open triangles).

of EF-Tu over Phe-tRNA^{Phe} was used and the reaction was allowed to proceed for a short time (30 and 60 s). This permitted discrimination of the EF-Tu-dependent tRNA binding from the much slower EF-Tu-independent tRNA binding. α-Sarcin-treated mixture showed about 60% activity compared with the untreated control ribosomes. Considering that in this assay 50% of the ribosomes produced dipeptide and that 25% of the total population were intact ribosomes, α-sarcin-cleaved ribosomes had to be responsible for, at least 30% of the dipeptide signal. This indicated that cleavage of the SRL partially allowed ternary complex functionality although at a lower extent and probably with the rates of tRNA accommodation and peptide bond formation significantly affected, parameters not tested here.

To further analyze the binding of ternary complex, we used a centrifugal filtration method to separate free EF-Tu from EF-Tu bound to the ribosome (36). In order to stabilize the binding, a non-hydrolyzable GTP analog (GDPNP) or an inactive EF-Tu mutant (EF-Tu H84A) (40) were used in the binding assay. EF-Tu bound to the ribosome was analyzed by SDS–PAGE (Figure 3B). α-Sarcin-cleaved ribosomes could bind the GTPase inactive ternary complexes but at lower levels compared to the untreated ribosomes. Similarly, binding of EF-Tu•GDPNP was slightly reduced with α-sarcin-treated ribosomes. Overall, our results showed that cleavage of the SRL moderately reduced ternary complex binding and progress of the aminoacyl tRNA to the peptidyl transferase reaction.

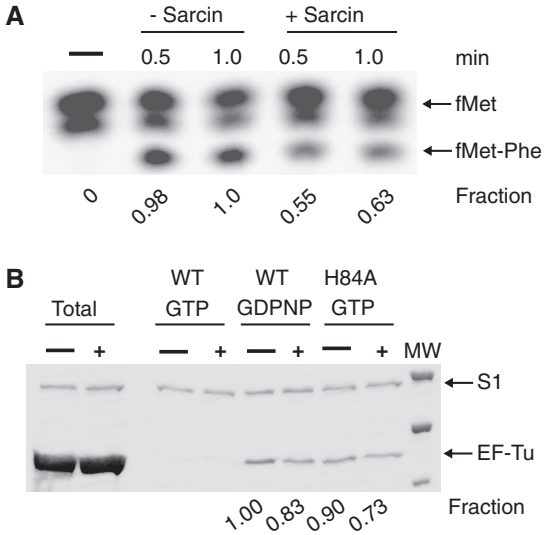

Figure 3. Binding of EF-Tu ternary complex to α-sarcin treated ribosomes. (**A**) Binding of EF-Tu•GTP•Phe-tRNA^{Phe} to the A site and peptide bond formation analyzed by electrophoretic TLC. Untreated control ribosomes (−Sarcin) and α-sarcin-treated ribosomes (+Sarcin) were incubated with EF-Tu ternary complex for the indicated time. The dipeptide formed (fMet-Phe) is indicated by the arrow. Normalized value of dipeptide formed is indicated below the lanes. (**B**) Binding of EF-Tu ternary complex to ribosomes analyzed by filtration and SDS-PAGE. WT or H84A mutant EF-Tu was bound to the ribosome in the presence of GTP or GDPNP and kirromycin. Control untreated ribosomes and α-sarcin-treated ribosomes are indicated by (–) and (+), respectively. Lanes: Total, samples before filtration; MW, protein molecular weight standards of 75, 50 and 37 KDa. The position of EF-Tu and the ribosomal protein S1 are indicated by arrows. Normalized value of EF-Tu bound to the ribosome is indicated below the lanes.

Translocation catalyzed by EF-G is drastically inhibited by cleaving the SRL

The effect of cleaving the SRL with α-sarcin on EF-G-dependent translocation was next analyzed. Pre-translocation complexes were formed with either deacylated or aminoacylated tRNAs in the P and A sites. Toeprinting assay showed that α-sarcin-treated ribosomes formed pre-translocation complexes with similar efficiency as control ribosomes (Figure 4A). Translocation was triggered by adding a large excess of EF-G•GTP to the pre-translocation complex and the movement of the mRNA–tRNA complex was monitored by the toeprinting assay (31). Untreated ribosomes translocated efficiently; in contrast, α-sarcin-treated ribosomes translocated poorly (Figure 4A). The background translocation observed could be attributed to the small amount of intact ribosomes present after α-sarcin treatment. Consistent with this idea, increasing the amount of tRNAs, EF-G•GTP or time of the reaction did not improve the extent of translocation (data not shown).

We corroborated this result with another, fluorescence-based, assay to monitor EF-G-dependent translocation (27). In this assay, translocation of the mRNA–tRNA complex causes a decrease in the fluorescence intensity of the pyrene probe attached to the 3′-end of a synthetic mRNA. Again, α-sarcin-treated ribosomes showed only a small decrease in the fluorescence intensity compared with the untreated control ribosomes in the presence of a large excess of EF-G (Figure 4B). The small decrease in the fluorescence intensity correlated with the amount of intact ribosomes present after treatment with α-sarcin. Thus, both the toeprinting data and the fluorescence-based assay for translocation showed that cleavage of the SRL strongly inhibited EF-G-dependent translocation.

To identify the step(s) in translocation that was inhibited by cleavage of the SRL, we tested EF-G-independent translocation. The antibiotic sparsomycin can induce translocation of the mRNA–tRNA complex, albeit at a slower rate than EF-G (34). Sparsomycin-dependent translocation was monitored by the toeprinting assay (Figure 5). Ribosomes treated with α-sarcin showed the same rate of translocation as the untreated control ribosomes. In contrast, experiments done in parallel to monitor the time course of EF-G-dependent translocation show significant inhibition with the α-sarcin-treated ribosomes (Figure 5). These results suggested that the movement of the mRNA–tRNA within the ribosome was not affected by cleaving the SRL, but some step(s) specific to the EF-G catalyzed process was inhibited.

EF-G binding and GTPase activity are impaired by the cleavage of the SRL

Binding of EF-G to the ribosome was next tested using the filtration method described above for EF-Tu. Stable EF-G binding was observed with GDPNP and the untreated ribosomes (Figure 6A). In contrast, reduced EF-G binding was observed with the α-sarcin-treated ribosomes, which was consistent with the background of intact ribosomes. Increasing the ratio of EF-G over ribosomes did not improve binding (data not shown). Thus, cleavage of the SRL considerably reduced the affinity of EF-G for the ribosome.

Finally, we tested the ability of EF-G to hydrolyze GTP in the presence of vacant ribosomes (Figure 6B). Time-course experiments were performed under multiple turnover conditions with untreated and α-sarcin-treated ribosomes mixed with varying concentrations of EF-G. The kinetic constants were extracted from the study of the dependence of initial velocities of GTP hydrolysis versus EF-G concentration of three independent experiments (35,40–42). Parameters for the SRL cleaved ribosomes were calculated by taking into account the presence of 25% intact ribosomes after α-sarcin treatment (see 'Materials and Methods' section) (35). We observed almost a 50-fold defect in k_{cat}/K_M for GTP hydrolysis by EF-G with the SRL cleaved ribosomes (Table 1). Although the experimental data showed substantial error values, especially in K_M, a dramatic defect in GTP hydrolysis was observed when ribosomes were treated with α-sarcin (Figure 6B). This defect in GTPase activity is consistent with the impaired binding of EF-G to the SRL cleaved ribosomes.

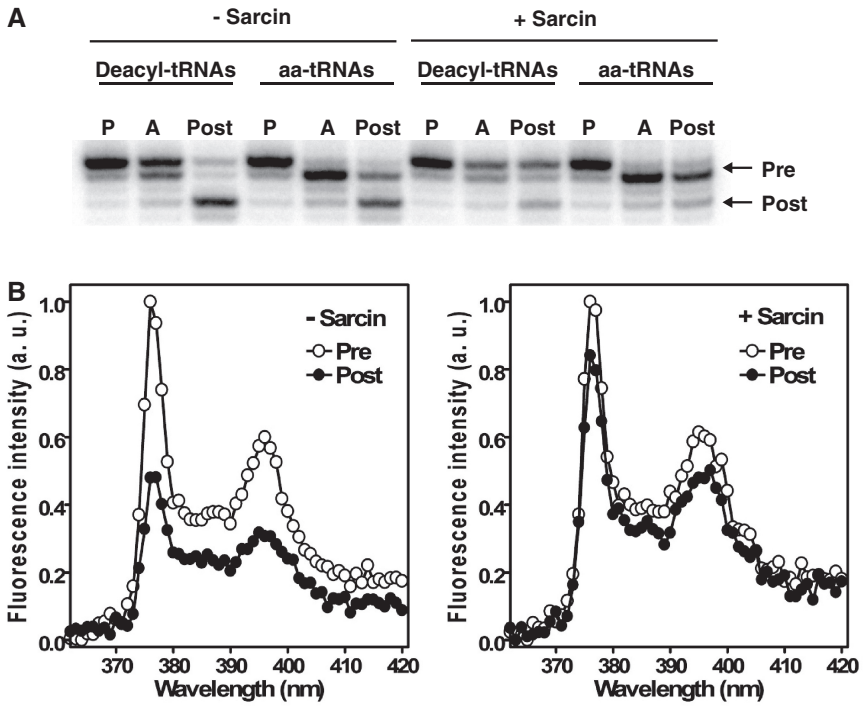

Figure 4. EF-G-dependent translocation. (**A**) Toeprinting analysis of translocation. Untreated control ribosomes (−Sarcin) and α-sarcin-treated ribosomes (+Sarcin) were incubated with mRNA and either deacylated tRNAs (deacyl-tRNAs) or aminoacylated tRNAs (aa-tRNAs) to form pre-translocation complexes. Lanes: P, ribosome with $tRNA^{fMet}$ in P site; A, pre-translocation complex with $tRNA^{fMet}$ in the P and $tRNA^{Phe}$ in the A site; Post, post-translocation complex formed by the addition of EF-G•GTP to the pre-translocation complex. The toeprints corresponding to the pre-translocation complex (Pre) and the post-translocation complex (Post) are indicated by the arrows. (**B**) Translocation monitored by a fluorescence-based assay. Pre-translocation complex contained fMet-$tRNA^{fMet}$ in the P site and Phe-$tRNA^{Phe}$ in the A site. Post-translocation complex was formed by incubating the pre-translocation complex with EF-G and GTP. Emission spectra of pre- (open circles) and post-translocation complexes (closed circles). The decrease in pyrene emission at 376 nm was used to quantify the extent of EF-G-dependent translocation. Left panel, untreated control ribosomes; right panel, α-sarcin-treated ribosomes.

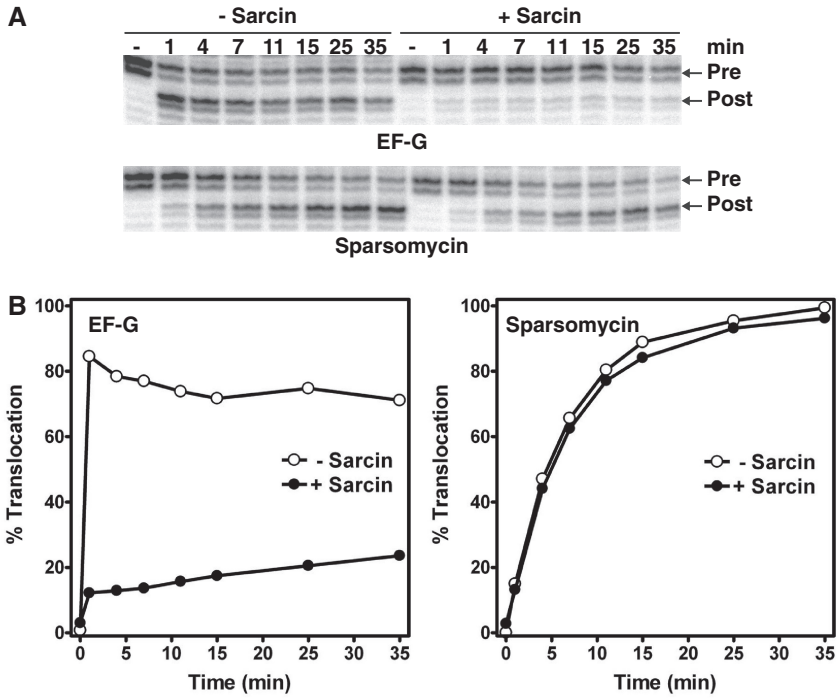

Figure 5. Sparsomycin-dependent translocation. (**A**) Time courses of translocation induced by EF-G (upper panel) or sparsomycin (lower panel), analyzed by toeprinting. Pre- and post-translocation toeprint bands are indicated by arrows. –lane, no EF-G or sparsomycin added; −Sarcin, untreated ribosomes; +Sarcin, α-sarcin-treated ribosomes. (**B**) Graphical representation of data in (A). Data were normalized to the maximum translocation value for untreated ribosomes. Open circles, untreated ribosomes; closed circles, ribosomes treated with α-sarcin. Left panel, EF-G-dependent translocation; right panel, sparsomycin-dependent translocation.

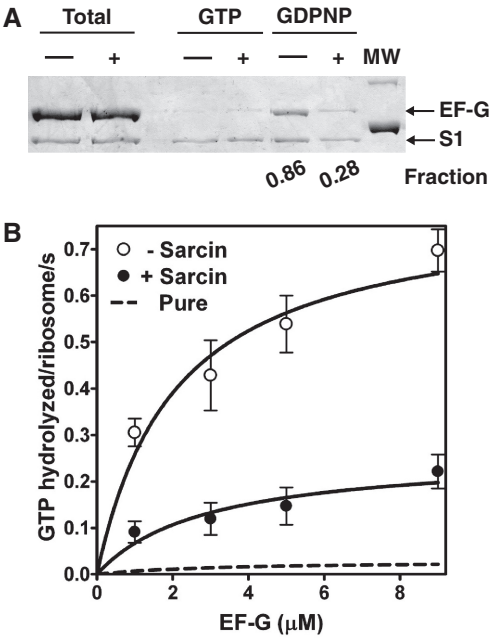

Figure 6. Interaction of EF-G with the ribosome. (**A**) Binding of EF-G to vacant ribosomes analyzed by filtration and SDS–PAGE. EF-G in the presence of GTP or GDPNP was used. (–), untreated ribosomes; (+), α-sarcin-treated ribosomes. Total indicates samples before separating unbound proteins. MW indicates protein standards of 100 and 75 KDa. The position of EF-G and ribosomal protein S1 are indicated by arrows. EF-G fraction bound to ribosomes is indicated below the lanes. (**B**) Rate of GTP hydrolysis versus EF-G concentration. Open circles, untreated ribosomes; closed circles, α-sarcin-treated ribosomes. Three independent experiments were averaged and the data fitted to a Michaelis–Menten equation. Dotted curve is theoretically obtained from the calculated kinetic constants in Table 1 for a population containing only cleaved ribosomes (Pure).

Table 1. GTP hydrolysis by EF-G in vacant ribosomes

Ribosome	k_{cat} (s^{-1})	K_M (μM)	k_{cat}/K_M ($\mu M^{-1} s^{-1}$)
−Sarcin	0.80 ± 0.12	2.08 ± 0.94	0.38
+Sarcin	0.26 ± 0.09	2.90 ± 2.55	0.09
Pure	0.03	3.41	0.008

−Sarcin, ribosomes not treated with α-sarcin. +Sarcin, ribosomes treated with α-sarcin, having 25% of intact ribosomes. Pure, kinetic constants calculated for a pure population of cleaved ribosomes (33).

DISCUSSION

Ribotoxins are an interesting family of enzymes due to their powerful and deadly activity against numerous types of living cells. Besides their ability of reaching the cytoplasm, the ribosome inactivation that results from their ribonucleolytic activity has stimulated extensive research in the field.

Prokaryotic SRL cleavage by α-sarcin

Ribotoxins seem to differently affect ribosomes from diverse origins even with the conserved SRL as the substrate (1,2). It has been proposed that the presence of C2666 instead of the corresponding eukaryotic G at the equivalent SRL position might explain the lower susceptibility of *E. coli* ribosomes against α-sarcin cleavage. Previous studies with small synthetic oligoribonucleotides mimicking the SRL sequence have suggested that there are at least two SRL areas that are recognized by this toxin, the GAGA tetraloop and the bulged G2655 (Figure 1A), indicating that the primary determinant for recognition is, more than the sequence, the SRL conformation (43–46). In fact, a recent study with synthetic SRL showed a cleavage-resistant population of the substrate that had a different conformation (39). Furthermore, crystal structures with different analogs that mimicked the SRL revealed that the residue equivalent to A2662 docked in the active site of the ribotoxin instead of the expected G2661, leading the authors to propose an alternative pathway for cleavage (47).

Our observation that two contiguous phosphodiester bonds within the prokaryotic SRL are susceptible to the action of the toxin (Figure 1C), not only agrees with previously published data, but also reveals that the recognition of intact ribosomes by ribotoxins might be more complex. In fact, a recent hypothesis focuses on the ability of ribotoxins to interact with other elements of the ribosomal machinery, such as the proteins L6 and L14, in order to access the SRL (48,49). In addition, electrostatics has an essential role in locating the ribotoxin on the ribosome surface contributing to its high affinity (38). In this study, relaxed specificity of ribotoxins was observed when trying to improve their activity against prokaryotic ribosomes by using certain conditions of magnesium and polyamines concentration. These counter ions directly affect the stability and conformation of the ribosomes, which could be the cause for the second cleavage site in the SRL by α-sarcin.

Effect of SRL cleavage on EF-G-dependent translocation

The SRL is not essential for factor-independent peptide synthesis (50). In contrast, elongation factor-related functions have been observed to be defective after ribotoxin treatment of different ribosomes. In general, the poor binding of either EF-Tu ternary complex or EF-G (or their eukaryotic homologs) was the main defect in the targeted ribosomes (4,51–53). In a more recent study, a single-molecule based analysis showed that cleavage of the SRL allowed initial binding and GTPase activation by EF-Tu ternary complex but blocked further progress to the accommodation step (25). These interesting results motivated us to examine whether EF-G can also transiently interact with the SRL-cleaved ribosome and activate GTP hydrolysis.

Translocation catalyzed by EF-G consists of many sub-steps that are not fully understood (11,54–56). Binding of EF-G•GTP to the ribosome induces a ratchet-like rotation of the small subunit relative to the large subunit and stabilizes the P and A site tRNAs in the P/E and A/P hybrid states (14,56). This is followed by GTP hydrolysis and conformational changes in the ribosome, which allow the rapid movement of the mRNA–tRNA complex (57,58). After translocation, the ribosome undergoes additional conformational changes and EF-G•GDP dissociates (58). Even though

the ribosome undergoes extensive structural rearrangements, the SRL maintains its interaction with EF-G in the pre- and post-translocation state (14,17,21,23,59). The SRL may, thus, play an important role in stabilizing the various transition states of EF-G during translocation. Interestingly, the SRL interacts intimately with the GTP-binding domain of EF-G implying a more direct role in catalyzing GTP hydrolysis (16,21,23).

We show that cleavage of the SRL inhibits EF-G-dependent translocation, while sparsomycin-dependent translocation is not affected (Figures 4 and 5). Therefore, in agreement with a previous report (4), the intrinsic ability of the ribosome to translocate tRNAs is not inhibited by cleaving the SRL. Moreover, sparsomycin-dependent translocation also requires the tRNAs to be in the hybrid state suggesting that a SRL cleaved ribosome can form this translation intermediate (60). Therefore, changes produced in the SRL once cleaved do not appear to have long-range effects, but mainly affect rapid translocation catalyzed by EF-G. Furthermore, our results show that cleavage of the SRL significantly impedes the binding of EF-G to the ribosome and therefore its GTP hydrolysis activity (Figure 6). We favor the idea that cleavage of the SRL inhibits translocation by blocking EF-G binding rather than by preventing GTP hydrolysis because previous studies have shown that slow translocation can occur even in the absence of GTP hydrolysis (55). Thus, it is unlikely that EF-G even progresses to the GTPase-activated state as opposed to the EF-Tu ternary complex (25). However, we cannot exclude the possibility that an initial binding complex is formed between the SRL-cleaved ribosome and EF-G•GTP that becomes unstable at some intermediate step during the progress to the GTPase-activated state.

The SRL interacts differently with EF-G and EF-Tu

In this study, binding of both elongation factors to the ribosome was analyzed and only EF-Tu could bind to ribosomes with the cleaved SRL (Figures 3 and 6), suggesting that they interact with the ribosome in a different conformation during the process of elongation. This is consistent with the single-molecule study that showed that EF-Tu ternary complex binds to unmodified ribosomes and SRL cleaved ribosomes with equal efficiency (25). According to these authors, the SRL cleaved ribosomes stall at the tRNA accommodation step after ternary complex binding. In our case, much longer times of dipeptide reaction give a significant fraction of accommodated tRNA, suggesting that this is a very slow reaction in the SRL-cleaved ribosome. Thus, initial binding of the EF-Tu ternary complex to the ribosome is not significantly affected by cleavage of the SRL, but subsequent events in tRNA selection are inhibited. This is markedly different from the effects on EF-G, which requires an intact SRL for stably binding to the ribosome. In agreement with this observation, other kinds of ribosome-inactivating proteins, the *N*-glycosidases, have been observed to differentially affect the function of elongation factors in a eukaryotic system by depurinating a specific base in the SRL (61). Finally, the antibiotic thiostrepton bound to the GAC does not affect the initial binding of EF-Tu ternary complex (25,62). In contrast, it weakens the interaction of EF-G with the ribosome by interacting with the GAC and L11 (41,63–65). The defect observed with a cleaved SRL appears very similar to thiostrepton suggesting that a network of interactions between GAC, SRL, L11 and EF-G are required for the stability of EF-G on the ribosome and for translocation.

These differences in interaction of the SRL with EF-Tu and EF-G may support the idea that the ribosome switches between two different conformational states to discriminate between the elongation factors (15,18). It has been shown that the SRL accessibility during elongation depends on the presence or absence of peptidyl-tRNA in the A site of the ribosome, representing the pre-translocation and post-translocation complexes, respectively (66). The SRL is located at the surface of the ribosome; however, it is not a very mobile structure and it does not present dramatic conformational changes when elongation factors are bound. It has been proposed that an important determinant for binding one factor or the other is the distance between the SRL and the GAC (18). From our results we can conclude that EF-G binding is more dependent on the SRL conformation than the EF-Tu ternary complex. Binding of the EF-Tu ternary complex may be stabilized by codon–anticodon interaction and other contacts with the ribosome, which may partially compensate for the loss of the SRL interaction. Very recent high-resolution crystal structures of the ribosome bound to EF-Tu ternary complex in the GTP transition state (22) or to EF-G in the post-translocation state (23), show very similar conformation of the SRL region with respect to both elongation factors (Figure 1C and D). However, our results suggest that the SRL is more important for the interaction of EF-G•GTP with the ribosome. During translocation the 30S subunit undergoes a ratchet-like rotation with respect to the 50S subunit (14). It is plausible that in the ratcheted state, the SRL may play a more important role in stabilizing EF-G•GTP on the ribosome. Following GTP hydrolysis and translocation, domain IV of EF-G moves into the decoding center forming additional interactions that stabilizes it on the ribosome (23). A high-resolution structure of EF-G•GTP bound to the ribosome in the pre-translocation state is needed to understand how the SRL stabilizes EF-G•GTP on the ribosome prior to GTP hydrolysis and translocation.

FUNDING

Project BFU 2006-04404 from the Ministerio de Educación y Ciencia (Spain) and a grant from the National Science Foundation (to S.J.). L.G.-O. and E.A.-G. are recipients of fellowships from the Ministerio de Educación y Ciencia (Spain). Funding for open access charge: National Science Foundation.

Conflict of interest statement. None declared.

REFERENCES

1. Lacadena,J., Alvarez-Garcia,E., Carreras-Sangra,N., Herrero-Galan,E., Alegre-Cebollada,J., Garcia-Ortega,L., Onaderra,M., Gavilanes,J.G. and Martinez del Pozo,A. (2007) Fungal ribotoxins: molecular dissection of a family of natural killers. *FEMS Microbiol. Rev.*, **31**, 212–237.
2. Schindler,D.G. and Davies,J.E. (1977) Specific cleavage of ribosomal RNA caused by alpha sarcin. *Nucleic Acids Res.*, **4**, 1097–1110.
3. Endo,Y. and Wool,I.G. (1982) The site of action of alpha-sarcin on eukaryotic ribosomes. The sequence at the alpha-sarcin cleavage site in 28 S ribosomal ribonucleic acid. *J. Biol. Chem.*, **257**, 9054–9060.
4. Hausner,T.P., Atmadja,J. and Nierhaus,K.H. (1987) Evidence that the G2661 region of 23S rRNA is located at the ribosomal binding sites of both elongation factors. *Biochimie*, **69**, 911–923.
5. Endo,Y., Mitsui,K., Motizuki,M. and Tsurugi,K. (1987) The mechanism of action of ricin and related toxic lectins on eukaryotic ribosomes. The site and the characteristics of the modification in 28S ribosomal RNA caused by the toxins. *J. Biol. Chem.*, **262**, 5908–5912.
6. Macbeth,M.R. and Wool,I.G. (1999) The phenotype of mutations of G2655 in the sarcin/ricin domain of 23S ribosomal RNA. *J. Mol. Biol.*, **285**, 965–975.
7. Chan,Y.L., Sitikov,A.S. and Wool,I.G. (2000) The phenotype of mutations of the base-pair C2658.G2663 that closes the tetraloop in the sarcin/ricin domain of *Escherichia coli* 23S ribosomal RNA. *J. Mol. Biol.*, **298**, 795–805.
8. Lancaster,L., Lambert,N.J., Maklan,E.J., Horan,L.H. and Noller,H.F. (2008) The sarcin–ricin loop of 23S rRNA is essential for assembly of the functional core of the 50S ribosomal subunit. *RNA*, **14**, 1999–2012.
9. Moazed,D., Robertson,J.M. and Noller,H.F. (1988) Interaction of elongation factors EF-G and EF-Tu with a conserved loop in 23S RNA. *Nature*, **334**, 362–364.
10. Schmeing,T.M. and Ramakrishnan,V. (2009) What recent ribosome structures have revealed about the mechanism of translation. *Nature*, **461**, 1234–1242.
11. Wintermeyer,W., Peske,F., Beringer,M., Gromadski,K.B., Savelsbergh,A. and Rodnina,M.V. (2004) Mechanisms of elongation on the ribosome: dynamics of a macromolecular machine. *Biochem. Soc. Trans.*, **32**, 733–737.
12. Pape,T., Wintermeyer,W. and Rodnina,M. (1999) Induced fit in initial selection and proofreading of aminoacyl-tRNA on the ribosome. *EMBO J.*, **18**, 3800–3807.
13. Rodnina,M.V., Savelsbergh,A., Katunin,V.I. and Wintermeyer,W. (1997) Hydrolysis of GTP by elongation factor G drives tRNA movement on the ribosome. *Nature*, **385**, 37–41.
14. Frank,J. and Agrawal,R.K. (2000) A ratchet-like inter-subunit reorganization of the ribosome during translocation. *Nature*, **406**, 318–322.
15. Valle,M., Zavialov,A., Sengupta,J., Rawat,U., Ehrenberg,M. and Frank,J. (2003) Locking and unlocking of ribosomal motions. *Cell*, **114**, 123–134.
16. Taylor,D.J., Nilsson,J., Merrill,A.R., Andersen,G.R., Nissen,P. and Frank,J. (2007) Structures of modified eEF2 80S ribosome complexes reveal the role of GTP hydrolysis in translocation. *EMBO J.*, **26**, 2421–2431.
17. Stark,H., Rodnina,M.V., Wieden,H.J., van Heel,M. and Wintermeyer,W. (2000) Large-scale movement of elongation factor G and extensive conformational change of the ribosome during translocation. *Cell*, **100**, 301–309.
18. Sergiev,P.V., Bogdanov,A.A. and Dontsova,O.A. (2005) How can elongation factors EF-G and EF-Tu discriminate the functional state of the ribosome using the same binding site? *FEBS Lett.*, **579**, 5439–5442.
19. Schuette,J.C., Murphy,F.V.T., Kelley,A.C., Weir,J.R., Giesebrecht,J., Connell,S.R., Loerke,J., Mielke,T., Zhang,W., Penczek,P.A. *et al.* (2009) GTPase activation of elongation factor EF-Tu by the ribosome during decoding. *EMBO J.*, **28**, 755–765.
20. Villa,E., Sengupta,J., Trabuco,L.G., LeBarron,J., Baxter,W.T., Shaikh,T.R., Grassucci,R.A., Nissen,P., Ehrenberg,M., Schulten,K. *et al.* (2009) Ribosome-induced changes in elongation factor Tu conformation control GTP hydrolysis. *Proc. Natl Acad. Sci. USA*, **106**, 1063–1068.
21. Connell,S.R., Takemoto,C., Wilson,D.N., Wang,H., Murayama,K., Terada,T., Shirouzu,M., Rost,M., Schuler,M., Giesebrecht,J. *et al.* (2007) Structural basis for interaction of the ribosome with the switch regions of GTP-bound elongation factors. *Mol. Cell*, **25**, 751–764.
22. Schmeing,T.M., Voorhees,R.M., Kelley,A.C., Gao,Y.G., Murphy,F.V.T., Weir,J.R. and Ramakrishnan,V. (2009) The crystal structure of the ribosome bound to EF-Tu and aminoacyl-tRNA. *Science*, **326**, 688–694.
23. Gao,Y.G., Selmer,M., Dunham,C.M., Weixlbaumer,A., Kelley,A.C. and Ramakrishnan,V. (2009) The structure of the ribosome with elongation factor G trapped in the post-translocational state. *Science*, **326**, 694–699.
24. Leonov,A.A., Sergiev,P.V., Bogdanov,A.A., Brimacombe,R. and Dontsova,O.A. (2003) Affinity purification of ribosomes with a lethal G2655C mutation in 23S rRNA that affects the translocation. *J. Biol. Chem.*, **278**, 25664–25670.
25. Blanchard,S.C., Gonzalez,R.L., Kim,H.D., Chu,S. and Puglisi,J.D. (2004) tRNA selection and kinetic proofreading in translation. *Nat. Struct. Mol. Biol.*, **11**, 1008–1014.
26. Powers,T. and Noller,H.F. (1991) A functional pseudoknot in 16S ribosomal RNA. *EMBO J.*, **10**, 2203–2214.
27. Studer,S.M., Feinberg,J.S. and Joseph,S. (2003) Rapid Kinetic Analysis of EF-G-dependent mRNA Translocation in the Ribosome. *J. Mol. Biol.*, **327**, 369–381.
28. Feinberg,J.S. and Joseph,S. (2006) Ribose 2′-hydroxyl groups in the 5′ strand of the acceptor arm of P-site tRNA are not essential for EF-G catalyzed translocation. *RNA*, **12**, 580–588.
29. Feinberg,J.S. and Joseph,S. (2001) Identification of molecular interactions between P site tRNA and the ribosome essential for translocation. *Proc. Natl Acad. Sci. USA*, **98**, 11120–11125.
30. Martinez-Ruiz,A., Garcia-Ortega,L., Kao,R., Lacadena,J., Onaderra,M., Mancheno,J.M., Davies,J., Martinez del Pozo,A. and Gavilanes,J.G. (2001) RNase U2 and alpha-sarcin: a study of relationships. *Meth. Enzymol.*, **341**, 335–351.
31. Bartetzko,A. and Nierhaus,K.H. (1988) Mg2 + /NH4 + /polyamine system for polyuridine-dependent polyphenylalanine synthesis with near *in vivo* characteristics. *Meth. Enzymol.*, **164**, 650–658.
32. Feinberg,J.S. and Joseph,S. (2006) A conserved base-pair between tRNA and 23S rRNA in the peptidyl transferase center is important for peptide release. *J. Mol. Biol.*, **364**, 1010–1020.
33. Joseph,S. and Noller,H.F. (1998) EF-G-catalyzed translocation of anticodon stem-loop analogs of transfer RNA in the ribosome. *EMBO J.*, **17**, 3478–3483.
34. Fredrick,K. and Noller,H.F. (2003) Catalysis of ribosomal translocation by sparsomycin. *Science*, **300**, 1159–1162.
35. Saarma,U., Remme,J., Ehrenberg,M. and Bilgin,N. (1997) An A to U transversion at position 1067 of 23 S rRNA from *Escherichia coli* impairs EF-Tu and EF-G function. *J. Mol. Biol.*, **272**, 327–335.
36. Wilson,K.S. and Nechifor,R. (2004) Interactions of translational factor EF-G with the bacterial ribosome before and after mRNA translocation. *J. Mol. Biol.*, **337**, 15–30.
37. Endo,Y., Huber,P.W. and Wool,I.G. (1983) The ribonuclease activity of the cytotoxin alpha-sarcin. The characteristics of the enzymatic activity of alpha-sarcin with ribosomes and ribonucleic acids as substrates. *J. Biol. Chem.*, **258**, 2662–2667.
38. Korennykh,A.V., Piccirilli,J.A. and Correll,C.C. (2006) The electrostatic character of the ribosomal surface enables extraordinarily rapid target location by ribotoxins. *Nat. Struct. Mol. Biol.*, **13**, 436–443.
39. Korennykh,A.V., Plantinga,M.J., Correll,C.C. and Piccirilli,J.A. (2007) Linkage between substrate recognition and catalysis during cleavage of sarcin/ricin loop RNA by restrictocin. *Biochemistry*, **46**, 12744–12756.
40. Daviter,T., Wieden,H.J. and Rodnina,M.V. (2003) Essential role of histidine 84 in elongation factor Tu for the chemical step of GTP hydrolysis on the ribosome. *J. Mol. Biol.*, **332**, 689–699.
41. Seo,H.S., Abedin,S., Kamp,D., Wilson,D.N., Nierhaus,K.H. and Cooperman,B.S. (2006) EF-G-dependent GTPase on the ribosome. conformational change and fusidic acid inhibition. *Biochemistry*, **45**, 2504–2514.

42. Nechifor,R., Murataliev,M. and Wilson,K.S. (2007) Functional interactions between the G′ subdomain of bacterial translation factor EF-G and ribosomal protein L7/L12. *J. Biol. Chem.*, **282**, 36998–37005.
43. Gluck,A. and Wool,I.G. (1996) Determination of the 28S ribosomal RNA identity element (G4319) for alpha-sarcin and the relationship of recognition to the selection of the catalytic site. *J. Mol. Biol.*, **256**, 838–848.
44. Correll,C.C., Wool,I.G. and Munishkin,A. (1999) The two faces of the *Escherichia coli* 23S rRNA sarcin/ricin domain: the structure at 1.11 A resolution. *J. Mol. Biol.*, **292**, 275–287.
45. Perez-Canadillas,J.M., Santoro,J., Campos-Olivas,R., Lacadena,J., Martinez del Pozo,A., Gavilanes,J.G., Rico,M. and Bruix,M. (2000) The highly refined solution structure of the cytotoxic ribonuclease alpha-sarcin reveals the structural requirements for substrate recognition and ribonucleolytic activity. *J. Mol. Biol.*, **299**, 1061–1073.
46. Correll,C.C., Beneken,J., Plantinga,M.J., Lubbers,M. and Chan,Y.L. (2003) The common and the distinctive features of the bulged-G motif based on a 1.04 A resolution RNA structure. *Nucleic Acids Res.*, **31**, 6806–6818.
47. Yang,X., Gerczei,T., Glover,L.T. and Correll,C.C. (2001) Crystal structures of restrictocin-inhibitor complexes with implications for RNA recognition and base flipping. *Nat. Struct. Biol.*, **8**, 968–973.
48. Garcia-Ortega,L., Masip,M., Mancheno,J.M., Onaderra,M., Lizarbe,M.A., Garcia-Mayoral,M.F., Bruix,M., Martinez del Pozo,A. and Gavilanes,J.G. (2002) Deletion of the NH2-terminal beta-hairpin of the ribotoxin alpha-sarcin produces a nontoxic but active ribonuclease. *J. Biol. Chem.*, **277**, 18632–18639.
49. Garcia-Mayoral,F., Garcia-Ortega,L., Alvarez-Garcia,E., Bruix,M., Gavilanes,J.G. and del Pozo,A.M. (2005) Modeling the highly specific ribotoxin recognition of ribosomes. *FEBS Lett.*, **579**, 6859–6864.
50. Chan,Y.L. and Wool,I.G. (2008) The integrity of the sarcin/ricin domain of 23S ribosomal RNA is not required for elongation factor-independent peptide synthesis. *J. Mol. Biol.*, **378**, 12–19.
51. Fernandez-Puentes,C. and Vazquez,D. (1977) Effects of some proteins that inactivate the eukaryotic ribosome. *FEBS Lett.*, **78**, 143–146.
52. Brigotti,M., Rambelli,F., Zamboni,M., Montanaro,L. and Sperti,S. (1989) Effect of alpha-sarcin and ribosome-inactivating proteins on the interaction of elongation factors with ribosomes. *Biochem. J.*, **257**, 723–727.
53. Nierhaus,K.H., Schilling-Bartetzko,S. and Twardowski,T. (1992) The two main states of the elongating ribosome and the role of the alpha-sarcin stem-loop structure of 23S RNA. *Biochimie*, **74**, 403–410.
54. Frank,J., Gao,H., Sengupta,J., Gao,N. and Taylor,D.J. (2007) The process of mRNA–tRNA translocation. *Proc. Natl Acad. Sci. USA*, **104**, 19671–19678.
55. Pan,D., Kirillov,S.V. and Cooperman,B.S. (2007) Kinetically competent intermediates in the translocation step of protein synthesis. *Mol. Cell*, **25**, 519–529.
56. Spiegel,P.C., Ermolenko,D.N. and Noller,H.F. (2007) Elongation factor G stabilizes the hybrid-state conformation of the 70S ribosome. *RNA*, **13**, 1473–1482.
57. Katunin,V.I., Savelsbergh,A., Rodnina,M.V. and Wintermeyer,W. (2002) Coupling of GTP hydrolysis by elongation factor G to translocation and factor recycling on the ribosome. *Biochemistry*, **41**, 12806–12812.
58. Savelsbergh,A., Katunin,V.I., Mohr,D., Peske,F., Rodnina,M.V. and Wintermeyer,W. (2003) An elongation factor G-induced ribosome rearrangement precedes tRNA–mRNA translocation. *Mol. Cell*, **11**, 1517–1523.
59. Agrawal,R.K., Heagle,A.B., Penczek,P., Grassucci,R.A. and Frank,J. (1999) EF-G-dependent GTP hydrolysis induces translocation accompanied by large conformational changes in the 70S ribosome. *Nat. Struct. Biol.*, **6**, 643–647.
60. Dorner,S., Brunelle,J.L., Sharma,D. and Green,R. (2006) The hybrid state of tRNA binding is an authentic translation elongation intermediate. *Nat. Struct. Mol. Biol.*, **13**, 234–241.
61. Xu,Y.Z. and Liu,W.Y. (2000) Effects of the active aldehyde group generated by RNA *N*-glycosidase in the sarcin/ricin domain of rat 28S ribosomal RNA on peptide elongation. *Biol. Chem.*, **381**, 113–119.
62. Gonzalez,R.L. Jr, Chu,S. and Puglisi,J.D. (2007) Thiostrepton inhibition of tRNA delivery to the ribosome. *RNA*, **13**, 2091–2097.
63. Rodnina,M.V., Savelsbergh,A., Matassova,N.B., Katunin,V.I., Semenkov,Y.P. and Wintermeyer,W. (1999) Thiostrepton inhibits the turnover but not the GTPase of elongation factor G on the ribosome. *Proc. Natl Acad. Sci. USA*, **96**, 9586–9590.
64. Cameron,D.M., Thompson,J., March,P.E. and Dahlberg,A.E. (2002) Initiation factor IF2, thiostrepton and micrococcin prevent the binding of elongation factor G to the *Escherichia coli* ribosome. *J. Mol. Biol.*, **319**, 27–35.
65. Harms,J.M., Wilson,D.N., Schluenzen,F., Connell,S.R., Stachelhaus,T., Zaborowska,Z., Spahn,C.M. and Fucini,P. (2008) Translational regulation via L11: molecular switches on the ribosome turned on and off by thiostrepton and micrococcin. *Mol. Cell*, **30**, 26–38.
66. Yu,H., Chan,Y.L. and Wool,I.G. (2009) The identification of the determinants of the cyclic, sequential binding of elongation factors Tu and G to the ribosome. *J. Mol. Biol.*, **386**, 802–813.